Development/Plasticity/Repair

Loss of *syd-1* from R7 Neurons Disrupts Two Distinct Phases of Presynaptic Development

Scott Holbrook, Jennifer K. Finley, Eric L. Lyons, and Tory G. Herman
Institute of Molecular Biology, University of Oregon, Eugene, Oregon 97403

Genetic analyses in both worm and fly have identified the RhoGAP-like protein Syd-1 as a key positive regulator of presynaptic assembly. In worm, loss of *syd-1* can be fully rescued by overexpressing wild-type Liprin-α, suggesting that the primary function of Syd-1 in this process is to recruit Liprin-α. We show that loss of *syd-1* from *Drosophila* R7 photoreceptors causes two morphological defects that occur at distinct developmental time points. First, *syd-1* mutant R7 axons often fail to form terminal boutons in their normal M6 target layer. Later, those mutant axons that do contact M6 often project thin extensions beyond it. We find that the earlier defect coincides with a failure to localize synaptic vesicles, suggesting that it reflects a failure in presynaptic assembly. We then analyze the relationship between *syd-1* and *Liprin-α* in R7s. We find that loss of *Liprin-α* causes a stronger early R7 defect and provide a possible explanation for this disparity: we show that *Liprin-α* promotes Kinesin-3/Unc-104/Imac-mediated axon transport independently of Syd-1 and that Kinesin-3/Unc-104/Imac is required for normal R7 bouton formation. Unlike loss of *syd-1*, loss of *Liprin-α* does not cause late R7 extensions. We show that overexpressing *Liprin-α* partly rescues the early but not the late *syd-1* mutant R7 defect. We therefore conclude that the two defects are caused by distinct molecular mechanisms. We find that Trio overexpression rescues both *syd-1* defects and that *trio* and *syd-1* have similar loss- and gain-of-function phenotypes, suggesting that the primary function of Syd-1 in R7s may be to promote Trio activity.

Introduction

Synapse development is initiated by adhesion molecules that recruit presynaptic and postsynaptic components to the site of contact. The RhoGAP-like protein Syd-1 is among the earliest such components to be recruited presynaptically, and its loss disrupts the localization of multiple presynaptic proteins, including the scaffold Liprin-α (Hallam et al., 2002; Dai et al., 2006; Patel et al., 2006; Owald et al., 2010, 2012). In worm, loss of *syd-1* is rescued by overexpressing Liprin-α, suggesting that the primary function of Syd-1 may be to recruit or potentiate Liprin-α activity (Dai et al., 2006; Patel et al., 2006; Patel and Shen, 2009).

The R7 photoreceptor neurons in the *Drosophila* eye provide a genetically tractable system in which to study presynaptic development. Wild-type R7s extend their axons to the medulla, in which they eventually form presynaptic boutons in layer M6 (Ting et al., 2005). The best-studied synapses are those between motor neurons and muscle. Less is known about how neurons such as R7s form synapses onto other neurons. At both fly neuromuscular junction (NMJ) and in R7s, presynaptic development requires the LAR receptor phosphatase (Clandinin et al., 2001; Maurel-Zaffran et al., 2001; Kaufmann et al., 2002), its binding partners Liprin-α (Kaufmann et al., 2002; Hofmeyer et al., 2006) and Liprin-β (Astigarraga et al., 2010), and the guanine exchange factor (GEF) Trio (Astigarraga et al., 2010; Ball et al., 2010). However, the two systems use somewhat different molecular mechanisms (Hofmeyer and Treisman, 2009; Astigarraga et al., 2010), highlighting the importance of studying multiple synapse types. Disrupting members of the LAR/Liprin/Trio pathway in R7s causes two distinct phenotypes. (1) Loss of LAR or Liprin-α prevents R7 terminals from maintaining contact with M6, causing many axons instead to terminate in the M3–M5 layers (Clandinin et al., 2001; Maurel-Zaffran et al., 2001; Choe et al., 2006; Hofmeyer et al., 2006); late loss of the homophilic adhesion molecule N-cadherin (Ncad) also causes this phenotype (Lee et al., 2001; Nern et al., 2005; Ting et al., 2005). (2) In contrast, loss of Liprin-β or Trio causes R7 terminals to extend beyond M6 (Astigarraga et al., 2010). Despite this dichotomy, overexpressing Trio in R7s rescues loss of LAR, Liprin-α, or Liprin-β (Maurel-Zaffran et al., 2001; Astigarraga et al., 2010), suggesting that Trio acts downstream of these genes and that the two R7 phenotypes might simply be different manifestations of the same underlying defect: a destabilized interaction with M6 (Astigarraga et al., 2010).

However, here we show that loss of *syd-1* causes both R7 defects and that the two defects occur at separate developmental time points. The earlier failure to contact M6 correlates with a failure to localize synaptic vesicles (SVs) and can be partially rescued by Liprin-α overexpression, suggesting that part of the early role of Syd-1 is to promote presynaptic assembly by positively regulating Liprin-α. The later projection of extensions is not ameliorated by either Liprin-α or Liprin-β overexpression.

Received March 14, 2012; revised Sept. 17, 2012; accepted Oct. 5, 2012.

Author contributions: S.H., J.K.F., and T.G.H. designed research; S.H., J.K.F., E.L.L., and T.G.H. performed research; S.H., J.K.F., and T.G.H. analyzed data; T.G.H. wrote the paper.

This work was supported by institutional National Institutes of Health National Research Service Award Training Grant 5-T32-HD07348 (S.H.), a Burroughs-Wellcome Career Development Award (T.G.H.), and National Institutes of Health Grant R01 EY019694 (T.G.H.). We are deeply grateful to William Saxton, Angeline Lim, and other members of the Saxton laboratory for allowing us to use their expertise and laboratory facilities to perform the axon transport experiments. We also thank the Saxton laboratory as well as Jessica Treisman, Tom Schwarz, and the Bloomington *Drosophila* Stock Center for fly stocks.

Correspondence should be addressed to Dr. Tory G. Herman, Institute of Molecular Biology, University of Oregon, Eugene, OR 97403. E-mail: herman@molbio.uoregon.edu.

DOI:10.1523/JNEUROSCI.1350-12.2012

 0270-6474/12/3218101-11$15.00/0

However, Trio overexpression rescues both *syd-1* mutant R7 defects, suggesting that the primary function of Syd-1 during both phases of R7 terminal development is to potentiate Trio activity.

Materials and Methods

Genetics. Individual homozygous R7s were generated and labeled using *GMR–FLP* and mosaic analysis with a repressible cell marker (MARCM) (Lee and Luo, 1999; Lee et al., 2001); homozygous cells expressed either *UAS–Synaptotagmin* (*Syt*)*–GFP* or *UAS–mito–GFP* under the control of *actin* (*act*)*–Gal4* (flies containing the *UAS* constructs and *act–Gal4* were obtained from the Bloomington *Drosophila* Stock Center). In each rescue experiment, the *UAS* construct to be tested was also present. Wholly homozygous retinas were generated using *ey3.5–FLP* (from Iris Salecker, Medical Research Council, London, UK) and techniques described in Stowers and Schwarz (1999). The animal in Figure 2, *F* and *F′*, is of genotype $norpA^{36}$*/Y; UAS–mito–GFP; PANR7–Gal4*. Mito–GFP was similarly enriched within the R7 terminals of wild-type animals of genotype *UAS–mito–GFP; PANR7–Gal4*.

The $syd\text{-}1^{w46}$ allele was induced by ethylmethane sulfonate mutagenesis of a wild-type *FRT82* chromosome and was mapped relative to DNA sequence polymorphisms between the *FRT82* and *rucuca* chromosomes using meiotic recombination (Berger et al., 2001). The $syd\text{-}1^{CD}$ allele was generated by FLP-induced recombination between the *FRT*-containing piggyBac insertions *PBac{WH}ferrochelatase*^{f02660} and *PBac{WH}RhoGAP100F*^{f04641} (Parks et al., 2004). The following mutations were also used: *Liprin-*α^{oos} (Hofmeyer et al., 2006), *Liprin-*α^{R60} (Kaufmann et al., 2002), $trio^{1}$ and $trio^{3}$ (Newsome et al., 2000), LAR^{2127} (Maurel-Zaffran et al., 2001), $imac^{170}$ (Pack-Chung et al., 2007), sev^{V1} (Mullins and Rubin, 1991), and $norpA^{36}$ (McKay et al., 1995; Riesgo-Escovar et al., 1995; Pearn et al., 1996). All animals used were raised at 25°C. All *norpA* and *sev* mutant animals analyzed were male; the developmental time course (see Fig. 5) and axon transport (see Fig. 4) analyses were performed with a mixture of males and females; all other experiments were performed with females.

Transgenes. The incomplete fly *syd-1* cDNA clone LD28013, the only one available at the time, was obtained from the *Drosophila* Genomics Resource Center and subcloned into the pGEM vector. The predicted missing 5′ region was amplified in several pieces from larval RNA by RT-PCR and appended to the incomplete cDNA. We were unable to amplify the first exon as predicted at the time and therefore synthesized the corresponding DNA sequence to complete our construction. This prediction has subsequently turned out to be incorrect: the N-terminal amino acid sequence MTVQPAEMA, encoded by our *syd-1* cDNA, is not found within any of the currently predicted Syd-1 isoforms. The remainder of our *syd-1* cDNA encodes the Syd-1 C isoform, whose N terminus, however, contains the amino acid sequence MCDSATTGCFLTRSSHR in place of our incorrect N-terminal sequence. We removed the stop codon from our assembled *syd-1* cDNA and subcloned it into a UAST vector containing a C-terminal FLAG tag. The final *UAS–syd-1–FLAG* construct was sequenced to ensure that it contained no mutations and, as shown in Figure 2, *E* and *F*, does fully rescue the *syd-1* mutant R7 defect.

In addition to the transgenes used in the *GMR–FLP*/MARCM experiments (mentioned above), we also used the following: *UAS–trio* (Bloomington *Drosophila* Stock Center), *UAS–HA–Liprin-*α (Hofmeyer et al., 2006), *UAS–HA–Liprin-*β (Astigarraga et al., 2010), *UAS–ANF–GFP* (Rao et al., 2001), *PANR7–Gal4* (Wernet et al., 2006), *UAS–N-synaptobrevin–GFP* (Zhang et al., 2002), *D42–Gal4* (Yeh et al., 1995), and *OK371–Gal4* (Mahr and Aberle, 2006).

Image acquisition and analysis: R7s. Brains were dissected, fixed, and stained as described previously (Miller et al., 2008). The localization of Syt–GFP and Mito–GFP in R7s was analyzed in adults ≤12 h after eclosion; each marker is more diffusely distributed in R7 axons of adults that are older than 1 d old (data not shown). We used the following antibodies: mouse anti-Chaoptin (24B10; 1:200) from the Developmental Studies Hybridoma Bank and rabbit anti-GFP (1:5000), anti-rabbit Alexa Fluor-488 (1:250), and anti-mouse Alexa Fluor-555 (1:250) from Invitrogen. Confocal images were collected on a Leica SP2 microscope and analyzed with Leica or Fiji software (http://fiji.sc/Fiji; Schindelin et al., 2012). All quantifications were performed blind. The "% R7s that fail to contact M6" = 100 × (homozygous R7s that fail to contact M6)/(all homozygous R7s). The "% R7s with extensions" = 100 × (homozygous R7s with extensions)/(all homozygous R7s). The "% of total extensions" = 100 × (homozygous R7s with extensions in the specified orientation)/(all homozygous R7s with extensions). sev^{V1} animals raised at 25°C have considerably fewer R7s than are present in wild type. In particular, we could score 76.7 ± 4.87 homozygous $syd\text{-}1^{CD}$ mutant R7s per otherwise wild-type brain but only 7.72 ± 0.68 homozygous $syd\text{-}1^{CD}$ mutant R7s per sev^{V1} mutant brain. As a consequence, there were only 1.80 ± 0.19 $syd\text{-}1^{CD}$ mutant R7s with extensions per sev^{V1} mutant brain (instead of the 19.0 ± 1.64 $syd\text{-}1^{CD}$ mutant R7s with extensions in each otherwise wild-type brain). We quantified the total percentages of stops and extensions for each sev^{V1} brain separately (see Fig. 2*E*,*F*; $n = 97$) but chose to bin multiple sev^{V1} brains together for the purpose of quantifying extension orientation (see Fig. 5*G*; $n = 7$). The binning was random: when the sev^{V1} brains were originally imaged, the data happened to be stored in seven separate folders; we simply binned together data within each folder. *t* tests were performed (one tailed for rescue experiments and for comparisons between wild type and mutant; two tailed for all other comparisons), and the resulting *p* values are provided.

Image acquisition and analysis: larval motor axons. Time-lapse imaging was performed in the laboratory of William Saxton at the University of California, Santa Cruz (Santa Cruz, CA). Wandering third-instar larvae were anesthetized as described by Moua et al. (2011). Imaging was initiated at 10–15 min and terminated at 25–30 min after anesthesia. Images were collected at two frames per second using a PerkinElmer Life and Analytical Sciences Ultraview spinning-disk confocal microscope. Data analyzed were from larvae that recovered from anesthesia and moved normally for at least 2 h after being returned to culture. Because *Liprin-*α is on chromosome 2, we used *D42–Gal4*, a neuron driver on chromosome 3, to drive ANF–GFP expression in *Liprin-*α mutants. Analogously, because *syd-1* is on chromosome 3, we used *OK371–Gal4*, a motor neuron driver on chromosome 2, to drive ANF–GFP expression in *syd-1* mutants. Images were analyzed with Fiji software (http://fiji.sc/Fiji; Schindelin et al., 2012). All quantifications were performed blind. Flux was calculated by analyzing the movements of fluorescent vesicles within a 20 μm region for 200 frames. One-tailed *t* tests were performed, and the resulting *p* values are provided.

Results

Loss of *syd-1* causes two defects in R7 axon terminal morphology

To identify genes required for presynaptic development, we performed a genetic screen using mosaic animals whose R7 neurons were homozygous for randomly mutagenized chromosomes (Lee et al., 2001). We specifically sought mutations that, like loss of Ncad, LAR, or Liprin-α, disrupted the ability of R7 axons to form terminal synaptic boutons in the M6 layer. We identified a single such mutation, *w46*, on chromosome 3R. Wild-type R7 axons terminate in ellipsoid boutons in the M6 layer of the medulla (Fig. 1*A*). In contrast, most *w46* mutant R7 axon terminals are reduced in size, and many fail to contact the M6 layer altogether (Fig. 1*B*). In addition, we noticed that *w46* mutant R7 terminals have a second phenotype, distinct from that caused by loss of Ncad, LAR, or Liprin-α: many of the terminals that do contact M6 project thin extensions either beyond or within it (Fig. 1*B*). These extensions vary in length and orientation, can branch, and often terminate in small, bouton-like varicosities. Mutations that cause R7s to adopt aspects of the R8 fate can cause their axons to lose contact with M6 (Morey et al., 2008). However, we found that *w46* mutant R7s express R7-specific and not R8-specific rhodopsins (data not shown), indicating that *w46* does not cause this fate transformation and instead specifically disrupts the connectivity of R7 axons.

We mapped *w46* by meiotic recombination to a small region that contains the fly homolog of the *Caenorhabditis elegans* gene

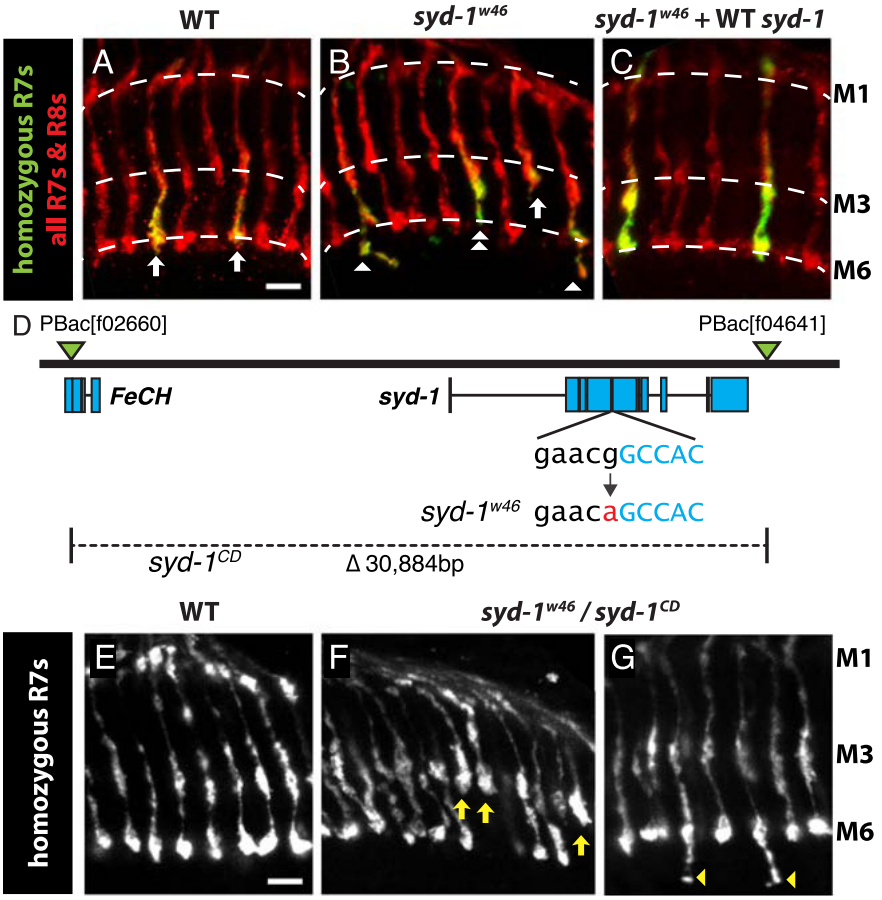

Figure 1. *syd-1* is required for normal R7 terminal bouton morphology. ***A–C***, Medullas of adult mosaic animals in which R7s homozygous for the specified chromosome arms express Syt–GFP (green). All R7 and R8 axons are labeled with mAb24B10 (red). Scale bar, 5 μm. ***A***, Each wild-type (*FRT82*) R7 axon terminates at the M6 layer in an ellipsoidal bouton (arrows). ***B***, *syd-1*^{w46} mutant R7 axons often fail to contact the M6 layer (arrow). Those that do contact M6 have abnormally small terminal boutons (double arrowhead), which often project thin extensions, many of which terminate in varicosities (arrowheads). ***C***, Expressing a *syd-1* cDNA in *syd-1*^{w46} mutant R7 axons rescues their morphological defects. ***D***, Schematic representation of the *syd-1* genomic region. The locations of the P elements used to create the *syd-1*^{CD} allele are indicated by green triangles. The locations of the *ferrochelatase* (*FeCH*) and *syd-1* exons are indicated by blue rectangles. The DNA sequence change in the *syd-1*^{w46} allele is indicated (exon sequence is in blue and intron in black), as is the extent of the *syd-1*^{CD} deletion. ***E–G***, Medullas of adult animals in which all R7 neurons are of the same genotype and are labeled with *PANR7–Gal4, UAS–N-synaptobrevin–GFP* (white). The *PANR7* promoter drives such high levels of expression that, despite being fused to an SV protein, GFP labels the whole R7 axon. Scale bar, 5 μm. ***E***, Wild-type (*FRT82*) R7s terminate in ellipsoid boutons at the M6 layer. ***F***, Like individual *syd-1*^{w46} mutant R7 axons, R7 axons in *syd-1*^{w46}/*syd-1*^{CD} mutant animals often fail to contact the M6 layer (arrows). ***G***, Like individual *syd-1*^{w46} mutant R7 axons, some R7 axon terminals in *syd-1*^{w46}/*syd-1*^{CD} mutant animals project thin extensions beyond M6 (arrowheads).

syd-1 (Hallam et al., 2002). We sequenced the *syd-1* locus within the *w46* mutant chromosome and found a single base-pair change within a 3′ splice site consensus sequence adjacent to the exon that is predicted to encode part of the RhoGAP homology domain (Fig. 1*D*). To test whether loss of *syd-1* was responsible for all observed defects in *w46* mutant R7 axon terminals, we caused the latter to express a wild-type *Drosophila syd-1* transgene (for details, see Materials and Methods). We found that this fully restored the morphology of *w46* mutant R7 terminals to wild type (Fig. 1*C*). We conclude that *syd-1* is required cell autonomously in R7s both to promote contact between their axon terminals and the M6 layer and to prevent the formation of extensions beyond that layer.

To test whether these phenotypes might be artifacts of creating individual *syd-1* mutant R7s, we next wanted to examine whole animals lacking *syd-1*. To do so, we generated a second allele of *syd-1* (which we refer to as *syd-1*^{CD}) by inducing recombination between *FRT*-containing transposons flanking the *syd-1* genomic region (Fig. 1*D*). We found that *syd-1*^{w46}/*syd-1*^{CD} transheterozygous adult animals have normal retinas and that their R7s display the same two axon terminal phenotypes as those described above: decreased contact with the M6 layer and extensions beyond M6 (Fig. 1*E–G*). We conclude that these defects are independent of our method of creating clones.

The *syd-1* and *Liprin-α* loss-of-function R7 phenotypes are not identical

In worm, loss of *syd-1* or *Liprin-α* causes indistinguishable defects in presynaptic development (Dai et al., 2006; Patel et al., 2006). In contrast, loss of *syd-1* from fly NMJ causes a smaller reduction in the number of active zones than does loss of *Liprin-α* (Owald et al., 2010), indicating that the latter may have *syd-1*-independent functions. In addition, loss of *syd-1* but not *Liprin-α* from fly NMJ causes postsynaptic defects, indicating that *syd-1* in turn has *Liprin-α*-independent functions (Owald et al., 2010, 2012). To investigate the relationship between *syd-1* and *Liprin-α* in R7s, we first compared their loss-of-function phenotypes.

syd-1^{CD} fully deletes *syd-1* and is therefore a null allele. However, *syd-1*^{CD} also removes most of a second gene, *ferrochelatase*, predicted to encode a mitochondrial enzyme required for the production of heme (Sellers et al., 1998). Because both *syd-1*^{CD} homozygotes and mosaic animals with entirely *syd-1*^{CD} homozygous retinas die before adulthood even when provided with wild-type *syd-1*, we conclude that loss of *ferrochelatase* is lethal—at least in combination with loss of *syd-1*—and that some vital tissue in addition to retina is rendered homozygous in the mosaic animals. Nonetheless, we were able to create individual *syd-1*^{CD} mutant R7s and found that they have the same defects as those caused by *syd-1*^{w46}: terminal boutons of reduced size in the M6 layer, failure to contact M6, and thin, sometimes branched, extensions that project beyond or within M6 (Fig. 2*A–C*). These defects are fully rescued by expression of a wild-type *syd-1* transgene within the *syd-1*^{CD} mutant R7s (Fig. 2*E*,*F*), indicating that none is caused by loss of *ferrochelatase*. However, the frequencies of the *syd-1*^{CD} R7 defects are slightly greater than that of *syd-1*^{w46} (Fig. 2*E*,*F*), indicating that the *w46* allele is non-null.

We next compared the *syd-1*^{CD} R7 defect with that caused by loss of *Liprin-α* and noted two striking differences: (1) a significantly greater proportion of *Liprin-α* than *syd-1* mutant R7 terminals fail to contact the M6 layer (Fig. 2*D*,*E*); and (2) consistent with previous reports (Astigarraga et al., 2010), *Liprin-α* mutant R7s do not project extensions either beyond or within M6 (Fig. 2*D*,*F*). Such differences might theoretically be observed if more wild-type Syd-1 than Liprin-α protein were to perdure in the

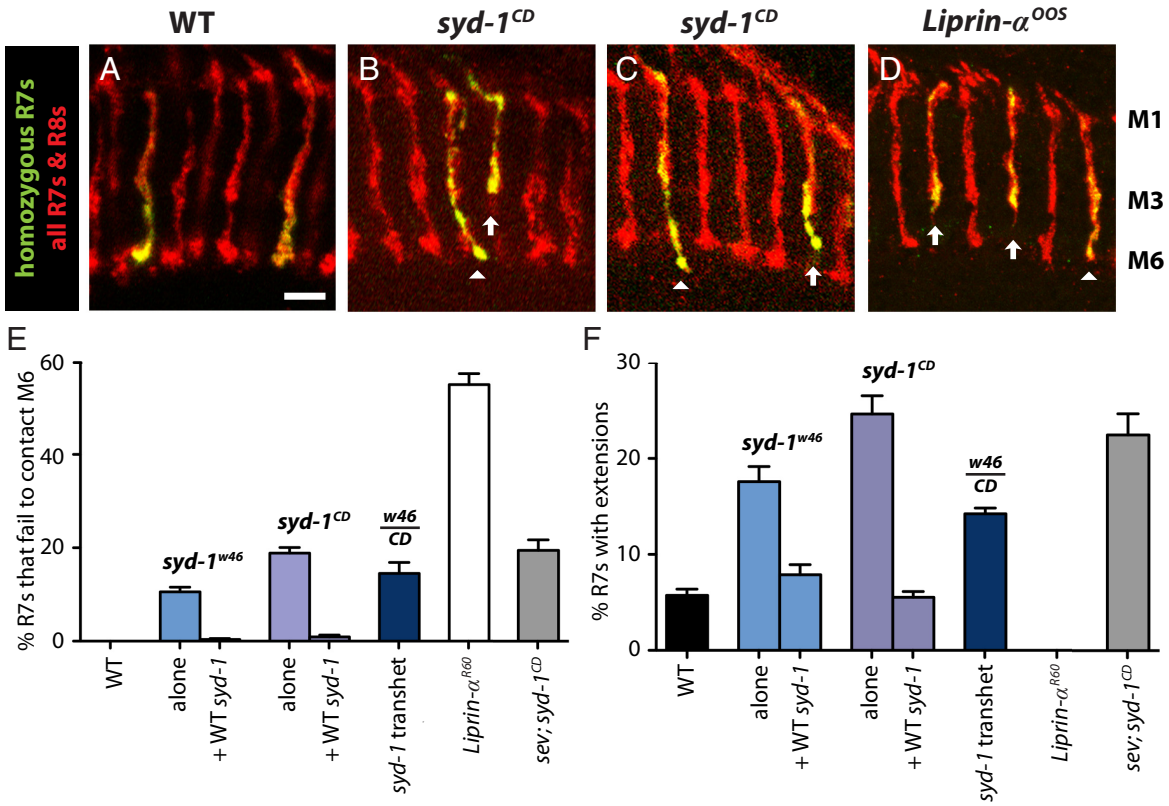

Figure 2. The *syd-1* and *Liprin-α* loss-of-function R7 phenotypes are not identical. ***A–D***, Medullas of adult mosaic animals in which homozygous R7s express Syt–GFP (green). All R7 and R8 axons are labeled with mAb24B10 (red). Scale bar, 5 μm. ***A***, Wild-type (*FRT82*) R7 axons. Like *syd-1*^{w46} mutant R7 axons, R7 axons homozygous for a deletion of *syd-1* (*syd-1*^{CD}) often fail to contact the M6 layer (***B***, ***C***, arrows). Those *syd-1*^{CD} axons that do contact M6 have abnormally small terminal boutons (***B***, arrowhead), which often project thin extensions beyond M6 (***C***, arrowhead). ***D***, *Liprin-α*^{R60} mutant R7 axons have abnormally small terminal boutons (arrowhead) and often fail to contact M6 (arrows), but their terminals do not have extensions. ***E***, The percentages of wild-type, *syd-1*, and *Liprin-α* mutant R7 axons that fail to contact M6. Error bars represent SEM. This *syd-1*^{w46} (10.6 ± 1.00%; $n = 16$ brains) and *syd-1*^{CD} (18.9 ± 1.25%; $n = 12$ brains) mutant R7 defect is rescued by expression of a wild-type *syd-1* cDNA (rescue of *syd-1*^{w46}, 0.393 ± 0.157%, $n = 9$ brains, $p < 0.0001$; rescue of *syd-1*^{CD}, 0.913 ± 0.433%, $n = 10$ brains, $p < 0.0001$). The difference between *syd-1*^{CD} and *syd-1*^{w46} is significant ($p < 0.0001$), as is the difference between *syd-1*^{CD} and *Liprin-α*^{R60} (55.0 ± 2.32%; $n = 9$ brains; $p < 0.0001$). The frequency with which R7s in *syd-1*^{w46}/*syd-1*^{CD} transheterozygous animals fail to contact M6 (14.5 ± 2.32%; $n = 7$ brains) is not significantly different from that of individual *syd-1*^{w46} mutant R7s ($p = 0.079$) or of individual *syd-1*^{CD} mutant R7s ($p = 0.086$). Removing adjacent R7s by means of a hypomorphic *sev* allele has no effect on the frequency with which *syd-1*^{CD} mutant R7s fail to contact M6 (19.5 ± 2.28%; $n = 97$ brains; $p = 0.93$). ***F***, The percentages of wild-type, *syd-1*, and *Liprin-α* mutant R7 axons that have extensions. Error bars represent SEM. Significantly greater percentages of *syd-1*^{w46} (17.6 ± 1.58%; $n = 16$ brains; $p < 0.0001$) and *syd-1*^{CD} (24.6 ± 1.89%; $n = 12$ brains; $p < 0.0001$) mutant R7 terminals have extensions than wild-type R7 terminals (5.75 ± 0.638%; $n = 15$ brains). This defect is rescued by expression of a wild-type *syd-1* cDNA (rescue of *syd-1*^{w46}, 7.89 ± 1.05%, $n = 9$ brains, $p < 0.0001$; rescue of *syd-1*^{CD}, 5.55 ± 0.584%, $n = 10$ brains, $p < 0.0001$). The difference between *syd-1*^{CD} and *syd-1*^{w46} is significant ($p = 0.0078$), as is the difference between *syd-1*^{CD} and *Liprin-α*^{R60} (0%; $n = 9$ brains; $p < 0.0001$). The frequency with which R7s in *syd-1*^{w46}/*syd-1*^{CD} transheterozygous animals have extensions (14.2 ± 0.59%; $n = 7$ brains) is not significantly different from that of individual *syd-1*^{w46} mutant R7s ($p = 0.19$) but is significantly less frequent than that of individual *syd-1*^{CD} mutant R7s ($p < 0.001$). Removing adjacent R7s by means of a *sev* mutation has no effect on the frequency with which *syd-1*^{CD} mutant R7 terminals have extensions (22.5 ± 2.19%; $n =$ 97 brains; $p = 0.73$).

corresponding individual mutant R7 clones. However, the defects of R7s in *syd-1*^{CD}/*syd-1*^{w46} animals are not significantly greater than those of individual *syd-1*^{w46} mutant R7s (Fig. 2*E*,*F*), indicating that wild-type Syd-1 does not perdure in individual *syd-1* mutant R7 clones. We therefore conclude that *Liprin-α* and *syd-1* function partly independently of one another during R7 terminal development.

To test the relationship between *Liprin-α* and *syd-1* further, we wanted to create *Liprin-α; syd-1* double-mutant R7s. Because *Liprin-α* and *syd-1* are on different chromosomes, it is technically difficult to create individual double-mutant R7s. Wholly *Liprin-α; syd-1* double-mutant animals die as embryos (Owald et al., 2010). We therefore set out to create mosaic animals whose entire retinas were doubly mutant. We found that retinas entirely homozygous for wild-type versions of both chromosome arms (*FRT40; FRT82*) are grossly normal, as are retinas doubly homozygous for either a *Liprin-α* mutation and a wild-type *syd-1* chromosome arm (*Liprin-α*^{R60}, *FRT40; FRT82*) or a wild-type *Liprin-α* chromosome arm and a *syd-1* mutation (*FRT40; FRT82, syd-1*^{w46}). However, retinas doubly mutant for *Liprin-α* and *syd-1* (*Liprin-α*^{R60}, *FRT40; FRT82, syd-1*^{w46}) are severely reduced in size, and the few remaining R neuron axons in the corresponding medullas are extremely disorganized (data not shown). We conclude that *Liprin-α* and *syd-1* have redundant roles during retina development, and these earlier roles prevent us from determining whether *Liprin-α* and *syd-1* might also have redundant roles in R7 axon terminal development. In the following sections, we describe additional approaches we took to examine the relationship between Liprin-α and Syd-1 during the development of R7 axon terminals.

Unlike loss of *Liprin-α*, loss of *syd-1* does not cause a gross defect in axon transport

syd-1 is required for the localization of Liprin-α to NMJ active zones (Owald et al., 2010), at which Liprin-α is thought to function as a scaffold that localizes additional presynaptic proteins

(for review, see Stryker and Johnson, 2007). Liprin-α has also been shown to bind Kinesin motor proteins and thereby promote anterograde axon transport of SVs (Shin et al., 2003; Miller et al., 2005; Wagner et al., 2009). We next wanted to test whether *syd-1* might similarly be required for normal axon transport or whether Liprin-α instead functions independently of Syd-1 in this process. To do so, we examined movement of the dense-core vesicle marker ANF–GFP in larval motor neuron axons. ANF–GFP particles are large and easy to follow, and their transport has been shown previously to require Kinesin-3/Unc-104/Imac (Barkus et al., 2008), a kinesin that Liprin-α has been shown to bind and regulate in worm (Wagner et al., 2009). We first tested our prediction that loss of *Liprin-α* would disrupt transport of ANF–GFP in *Drosophila* motor neuron axons. Indeed, we found that *Liprin-α* mutant animals have significantly fewer ANF–GFP particles moving in the anterograde direction (Fig. 3*A*). In contrast, ANF–GFP movement in *syd-1* mutant animals is indistinguishable from wild type (Fig. 3*A*), suggesting that Liprin-α can promote axon transport independently of Syd-1.

This result suggested a possible explanation for one of the differences between the *Liprin-α* and *syd-1* mutant R7 phenotypes. Because loss of Kinesin-3/Unc-104/Imac prevents presynaptic bouton development at fly NMJ (Pack-Chung et al., 2007), we hypothesized that the *Liprin-α*-specific defect in axon transport might contribute to the increased frequency with which *Liprin-α* mutant R7s fail to form boutons in M6. If so, we would predict that loss of Kinesin-3/Unc-104/Imac from R7s would disrupt the ability of R7s to form boutons in M6. Indeed, we found that individual *imac* mutant R7s often fail to contact M6 (Fig. 3*B*,*C*). We did not quantify this phenotype because *imac* mutant R7 axons frequently lack GFP, preventing us from unambiguously identifying them as such (Fig. 3*C* and data not shown).

Loss of *syd-1* nonetheless disrupts the enrichment of SVs and mitochondria at R7 axon terminals

In worm, both *Liprin-α* and *syd-1* are required for clustering of SVs at en passant synapses (Zhen and Jin, 1999; Hallam et al., 2002; Dai et al., 2006; Patel et al., 2006). To test whether *Liprin-α* and *syd-1* are similarly required for SV clustering at R7 terminal synapses, we used the SV marker Syt–GFP. We found that, in newly eclosed wild-type adults, Syt–GFP predominantly localizes to the region of R7 axons that spans layers M4–M6 of the medulla (Fig. 4*A*,*A′*); a smaller amount localizes to the M1 region of the R7 axon. This pattern is consistent with the known locations of presynaptic sites within R7s (Takemura et al., 2008), suggesting that Syt–GFP accurately reflects the localization of SVs. In contrast, even in *syd-1* and *Liprin-α* mutant R7 axons that contact the M6 target layer, Syt–GFP accumulates in broadly distributed puncta (Fig. 4*B*–*D′*). We conclude that, despite the difference between their effects on Kinesin-3/Unc-104/Imac-dependent axon transport [which includes transport of SVs (Pack-Chung et al., 2007; Barkus et al., 2008)], *syd-1* and *Liprin-α* are both required for clustering of SVs in R7 axon terminals.

In addition to active zone proteins and SVs, mitochondria are also enriched at presynaptic sites. We found that, like Syt–GFP, the mitochondrial marker Mito–GFP is enriched in wild-type R7 terminals (Fig. 4*E*,*E′*), suggesting that mitochondria are indeed associated with presynaptic sites in R7s. This association is independent of evoked synaptic activity, because Mito–GFP remains localized to the terminals of *norpA* mutant R7s, in which phototransduction is blocked (Fig. 4*F*,*F′*; Bloomquist et al., 1988; Pearn et al., 1996). In contrast, even in *syd-1* and *Liprin-α* mutant R7 axons that contact the M6 target layer, Mito–GFP is found in broadly distributed puncta (Fig. 4*G*–*H′*). We conclude that *syd-1* and *Liprin-α* are also required for the enrichment of mitochondria at R7 axon terminals. We note that the morphological defects of *syd-1* and *Liprin-α* mutant R7 terminals are unlikely to be an indirect consequence of mitochondrial mislocalization: Miro mutant R7 axon terminals, which completely lack mitochondria (Guo et al., 2005), have wild-type morphology (data not shown).

syd-1 mutant R7 terminals mislocalize SVs and lose contact with M6 during the first half of pupal development; only later do they project extensions

To understand the relationships among the *syd-1* mutant R7 defects, we next determined the time course of each. Decreased contact between R7 terminals and the M6 layer can be caused by

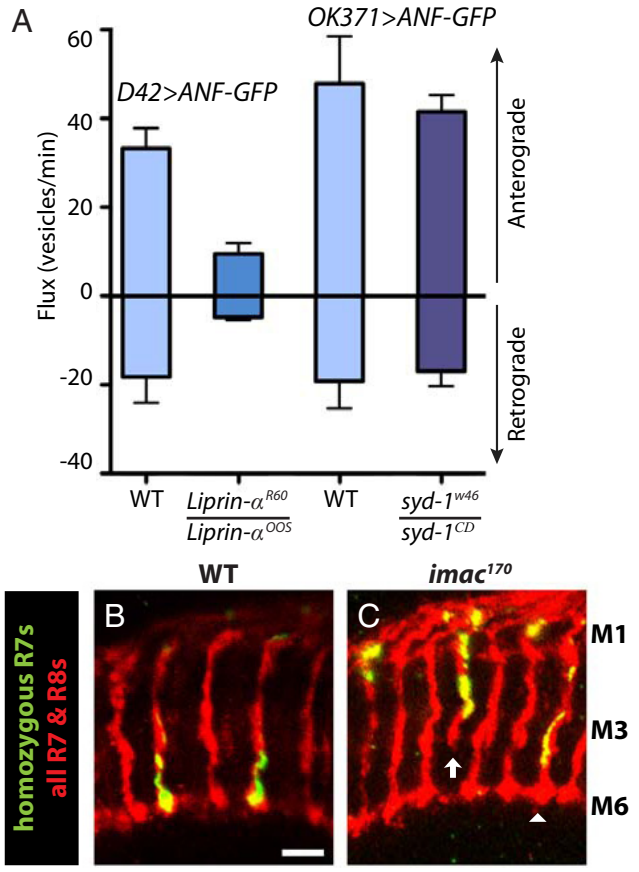

Figure 3. Loss of *Liprin-α* but not *syd-1* significantly disrupts axon transport, which is required for R7 axons to retain contact with M6. ***A***, The number of ANF–GFP-containing vesicles moving in the anterograde or retrograde direction within larval motor neurons of the indicated genotypes. Error bars represent SEM. In *Liprin-α* mutants, flux in the anterograde direction (9.48 ± 2.46 vesicles per minute; $n = 5$ larvae) is significantly different from that in the matched wild-type control (33.26 ± 4.54; $n = 7$ larvae; $p = 0.0011$). Flux in the retrograde direction also appears to differ between *Liprin-α* mutants (4.80 ± 0.66; $n = 5$ larvae) and wild type (18.26 ± 5.78; $n = 7$ larvae), but this difference is only marginally significant ($p = 0.041$). In *syd-1* mutants, flux in anterograde (41.52 ± 3.78; $n = 5$ larvae) and retrograde (16.92 ± 3.42; $n = 5$ larvae) directions is not significantly decreased compared with those in the matched wild-type control (anterograde, 47.85 ± 10.7, $n = 4$ larvae, $p = 0.28$; retrograde, 19.2 ± 6.1, $n = 4$ larvae, $p = 0.38$). ***B***, ***C***, Medullas of adult mosaic animals in which homozygous R7s express Mito–GFP (green). All R7 and R8 axons are labeled with mAb24B10 (red). Scale bar, 5 μm. Unlike wild-type (*FRT42*) R7 axons (***B***), *imac* mutant R7 axons often fail to contact the M6 layer (***C***, arrow). Mito–GFP is frequently mislocalized in or absent from *imac* mutant R7 axons (***C***, arrowhead indicates an *imac* mutant R7 axon that forms a terminal bouton in M6 from which Mito–GFP is nonetheless excluded).

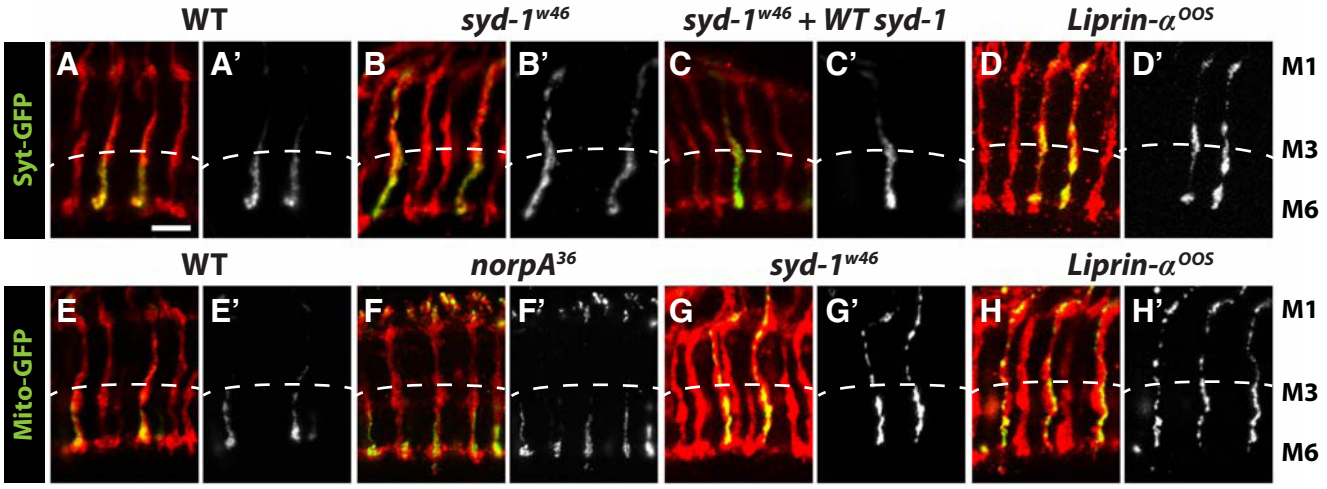

Figure 4. *syd-1* and *Liprin-α* are required for the enrichment of SVs and mitochondria at R7 terminals. ***A–D′***, Medullas of adult mosaic animals in which homozygous R7s express Syt–GFP (green). All R7 and R8 axons are labeled with mAb24B10 (red). Scale bar, 5 μm. In wild-type (*FRT82*) R7s, Syt–GFP is preferentially localized to the region of the axon that lies below the M3 layer (***A***, ***A′***), whereas in *syd-1*^{w46} mutant R7 axons, Syt–GFP is more broadly distributed and punctate (***B***, ***B′***). Syt–GFP is similarly mislocalized in *syd-1*^{CD} mutant R7s (data not shown). ***C***, ***C′***, Expressing a *syd-1* cDNA in *syd-1* mutant R7 axons results in normal localization of Syt–GFP. ***D***, ***D′***, Syt–GFP is similarly mislocalized and punctate in *Liprin-α* mutant R7 axons. ***E–H′***, Medullas of adult mosaic animals in which homozygous R7s express Mito–GFP (green). All R7 and R8 axons are labeled with mAb24B10 (red). ***E***, ***E′***, In wild-type (*FRT82*) R7s, Mito–GFP is preferentially localized to the region of the axon that lies below the M3 layer. ***F***, ***F′***, Mito–GFP remains enriched at R7 terminals even when phototransduction is disrupted by loss of *norpA*. Note that all R7s in this animal lack *norpA* and express Mito–GFP (see Materials and Methods). In contrast, in both *syd-1* (***G***, ***G′***) and *Liprin-α* (***H***, ***H′***) mutant R7 axons, Mito–GFP is broadly distributed and punctate. Expressing a *syd-1* cDNA in *syd-1* mutant R7 axons results in normal localization of Mito–GFP (data not shown).

at least two different mechanisms: (1) *Ncad* mutant R7 axons often fail to reach the temporary target layer in the medulla to which R7 axons initially project, and they appear to have collapsed growth cones (Ting et al., 2005), whereas (2) *LAR* and *Liprin-α* mutant R7 axons initially reach the temporary target layer and only later lose contact with it (Clandinin et al., 2001; Maurel-Zaffran et al., 2001; Ting et al., 2005; Hofmeyer et al., 2006). To distinguish whether, like *Liprin-α*, *syd-1* is not required for R7 axons to initially reach their targets, we examined *syd-1* mutant R7 axon terminals at 24 h after puparium formation (APF), a time point at which *Ncad* mutant R7s display a defect but *LAR* and *Liprin-α* mutant R7s do not (Ting et al., 2005; Hofmeyer et al., 2006). We found that wild-type and *syd-1* mutant R7 axons are indistinguishable at this stage (Fig. 5*A–B′*), indicating that *syd-1* is not required for R7 axons to reach their temporary target layer and does not affect the gross morphology of R7 terminals at this time point. In addition, the localization of Syt–GFP within wild-type and *syd-1* mutant R7 axons at this time is indistinguishable: most Syt–GFP is in the axon terminals (Fig. 5*A–B′*), suggesting that the later Syt–GFP puncta in *syd-1* mutant R7 axons may reflect a defect in retaining Syt–GFP within these terminals.

We next examined *syd-1* mutant R7 axon terminals at 55 h APF. Unlike wild-type R7 terminals at this stage (Fig. 5*C*,*C′*), *syd-1* mutant R7 terminals are abnormally small and often fail to contact the M6 layer, and Syt–GFP is mislocalized in broadly distributed puncta (Fig. 5*D*,*D′*). We conclude that, like *Liprin-α*, *syd-1* is required for the interaction between R7 terminals and their final target layer M6 and that both this interaction and the clustering of Syt–GFP at presynaptic sites within R7 terminals normally occur between 24 and 55 h APF.

By 55 h APF, the percentages of *syd-1*^{w46} and *syd-1*^{CD} mutant R7 axons that fail to contact M6 are maximal (Fig. 5*E*). However, *syd-1* mutant R7 terminals do not project extensions at this time point (Fig. 5*D*,*D′*,*F*). Instead, those *syd-1* mutant terminals that do contact M6 terminate in smooth boutons of reduced size (Fig. 5*D*,*D′*). We conclude that (1) the extensions observed in adult occur at a later time point than the failure to contact M6 and the mislocalization of Syt-GFP, and (2) the extensions are formed by an active process rather than by a failure to retract or remodel growth cone filopodia. By 72 h APF, the percentage of *syd-1*^{w46} mutant R7 terminals that have extensions is maximal and the percentage of *syd-1*^{CD} mutant R7 terminals with extensions is significantly greater than that in wild-type (Fig. 5*F*). We conclude that the extension process is initiated between 55 and 72 h APF and note that the infrequent R7 extensions observed in wild type also appear during this period.

Previous work has shown that R7 axon terminals are mutually repulsive (Ashley and Katz, 1994; Ting et al., 2007). We noticed that both wild-type and *syd-1* mutant R7 terminals project extensions primarily in the forward orientation (i.e., beyond the M6 layer) rather than laterally (i.e., within or parallel to M6; Fig. 5*G*). We therefore wondered whether these extensions were prevented from projecting laterally by repulsion from neighboring R7 terminals. To test this, we used a hypomorphic *sev* allele to eliminate most R7s (Mullins and Rubin, 1991). We found that those isolated *syd-1* mutant R7s that remain still fail to contact M6 (Fig. 2*E*) and project extensions (Fig. 2*F*) at the same frequencies and that the orientation of their extensions does not change (Fig. 5*G*). We conclude that *syd-1* mutant R7 extensions are unaffected by repulsion by neighboring R7 axons and instead have an intrinsic propensity to orient forward.

Overexpressing Liprin-α in *syd-1* mutant R7s restores their contact with the M6 layer but does not prevent the formation of extensions; overexpressing Liprin-β has no effect on *syd-1* mutant R7 terminals

In worm, loss of *syd-1* is fully rescued by *Liprin-α* overexpression, suggesting that the primary role of Syd-1 is to localize or otherwise activate Liprin-α (Dai et al., 2006; Patel et al., 2006; Patel and Shen, 2009). To test whether the same might be true in R7s, we used the *act* promotor to overexpress Liprin-α in individual *syd-1*^{CD} mutant R7s (the same methodology that we used to show that Syd-1 fully rescues *syd-1*^{CD} mutant R7s). We found that Liprin-α

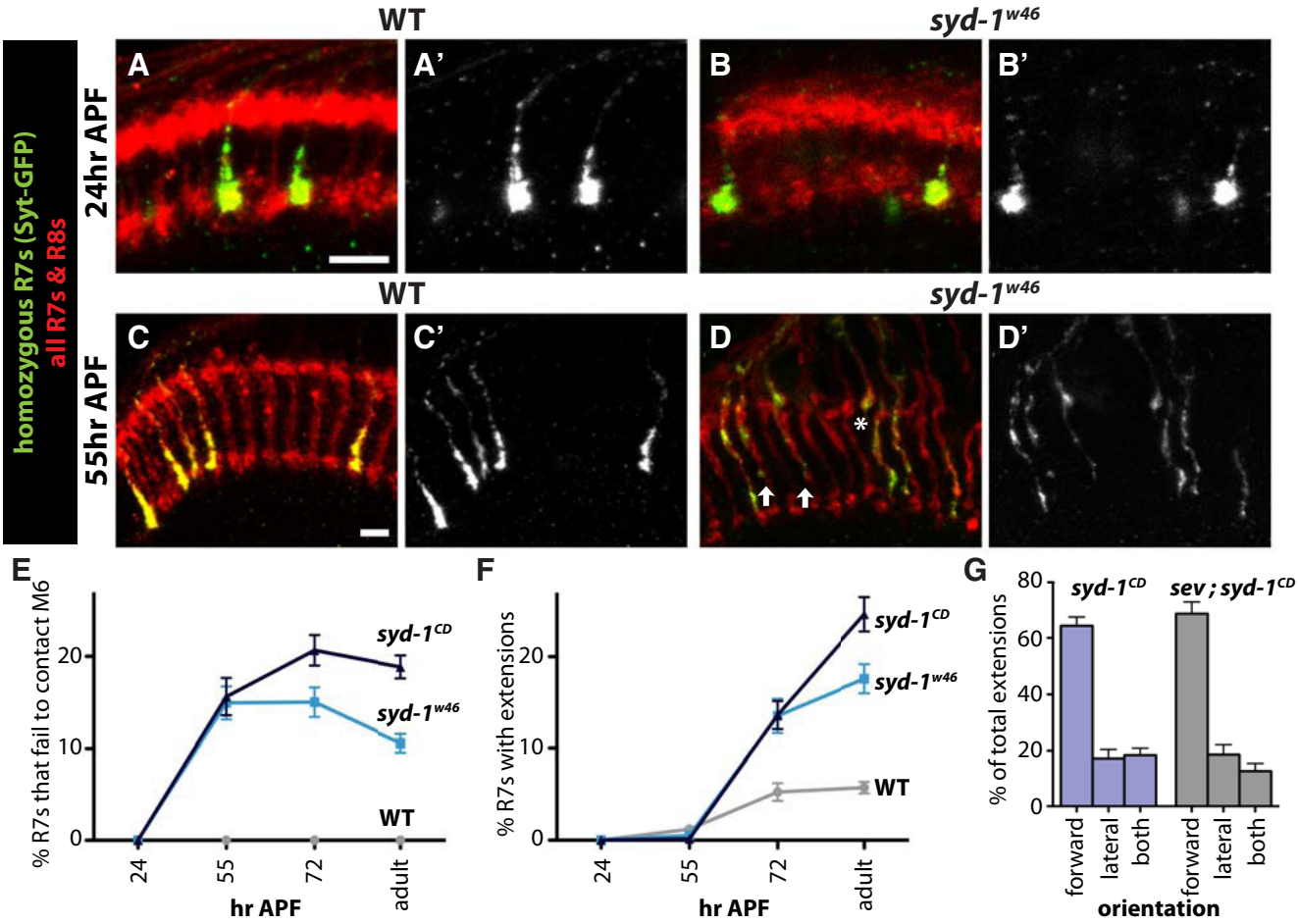

Figure 5. *syd-1* mutant R7 terminals first lose contact with M6 and only later project extensions. ***A–D'***, Medullas of mosaic pupae in which homozygous R7s express Syt–GFP (green). All R7 and R8 axons are labeled with mAb24B10 (red). Scale bars, 5 μm. At 24 h APF, wild-type (***A***, ***A'***) and *syd-1* mutant (***B***, ***B'***) R7 axons are indistinguishable: their growth cones have similar morphology, they terminate in the R7 target layer, and Syt–GFP is enriched within their terminals. By 55 h APF (***C–D'***), *syd-1* mutant R7 terminals often fail to contact the R7 target layer (***D***, arrows), those that do contact M6 have smaller boutons than wild type, and Syt–GFP is mislocalized and punctate. However, neither wild-type nor *syd-1* mutant R7 terminals have extensions at this time point. The asterisk in ***D*** indicates a *syd-1* mutant R7 axon that appears to terminate in M1 but that in fact extends to M6 in focal planes not included in this image. ***E***, The percentages of wild-type and *syd-1* mutant R7 axons that fail to contact the R7 target layer at 24, 55, and 72 h APF and in adult. Error bars represent SEM. At 24 h APF, all wild-type and *syd-1* mutant R7s contact the R7 target layer (wild type, $n = 5$ brains; *syd-1*^{w46}, $n = 9$ brains; *syd-1*^{CD}, $n = 10$ brains). However, by 55 h APF, 14.9 $\pm$ 1.80% ($n = 12$ brains) of *syd-1*^{w46} and 15.6% $\pm$ 2.03% ($n = 11$ brains) of *syd-1*^{CD} R7s no longer do so. The percentages of *syd-1* mutant R7 axons with this defect are not significantly different at 72 h APF (*syd-1*^{w46}, 15.0 $\pm$ 1.61%, $n = 12$ brains, $p = 0.97$; *syd-1*^{CD}, 20.7 $\pm$ 1.66%, $n = 12$ brains, $p = 0.067$), nor does the percentage of *syd-1*^{CD} mutant R7s with this defect change significantly between 72 h APF and adulthood [$p = 0.39$; the difference between the 55 h APF and adult percentages is also insignificant ($p = 0.18$)]. However, the percentage of *syd-1*^{w46} mutant R7s with this defect may decrease slightly between 72 h APF and adulthood [$p = 0.021$; the decrease between the 55 h APF and adult percentages is also marginally significant ($p = 0.032$)]. The adult data used are the same as that in Figure 2*E* and are redisplayed here for ease of comparison. ***F***, The percentages of wild-type and *syd-1* mutant R7 axon terminals that have extensions at 24, 55, and 72 h APF and in adult. Error bars represent SEM. At 24 h APF, wild-type and *syd-1* mutant R7 axon terminals are indistinguishable (wild type, $n = 5$ brains; *syd-1*^{w46}, $n = 9$ brains; *syd-1*^{CD}, $n = 10$ brains). By 55 h APF, a small percentage of wild-type R7s (1.20 $\pm$ 0.404%; $n = 12$ brains) have short extensions beyond their target layer. At this time point, the percentage of *syd-1*^{w46} mutant R7s with extensions (0.528 $\pm$ 0.276%; $n = 12$ brains) is not significantly different from that of wild type ($p = 0.18$), and the percentage of *syd-1*^{CD} mutant R7s with this defect (0.145 $\pm$ 0.15%; $n = 11$ brains) may be slightly lower than that of wild type ($p = 0.027$). By 72 h APF, a significantly greater percentage of *syd-1*^{w46} (13.5 $\pm$ 1.87%; $n = 12$ brains; $p < 0.001$) and *syd-1*^{CD} (13.6 $\pm$ 1.54%; $n = 12$ brains; $p < 0.0001$) mutant R7s have extensions than do wild-type R7s. The percentage of *syd-1*^{w46} mutant R7s with this defect does not change significantly between 72 h APF and adulthood ($p = 0.11$). However, the percentage of *syd-1*^{CD} mutant R7s with this defect increases significantly during this period ($p < 0.001$). The adult data used are the same as that in Figure 2*E* and are redisplayed here for ease of comparison. ***G***, Of those *syd-1*^{CD} mutant R7 axon terminals that have extensions, the percentages whose extensions project forward, laterally, or both (R7s with both have either a single extension that projects both forward and laterally or two extensions of which one projects forward and the other laterally). Removing adjacent R7s by means of a *sev* mutation has no significant effect on the orientation of *syd-1*^{CD} mutant R7 extensions [in the presence of neighboring R7s, 64.3 $\pm$ 3.14% extend forward, 17.3 $\pm$ 3.23% extend laterally, and 18.5 $\pm$ 2.49% have extensions in both directions ($n = 14$ brains); in the absence of neighboring R7s, 68.6 $\pm$ 4.15% extend forward ($p = 0.42$), 18.6 $\pm$ 3.56% extend laterally ($p = 0.79$), and 12.8 $\pm$ 2.71% have extensions in both directions ($p = 0.17$); $n = 7$ sets of data binned from multiple brains (for details, see Materials and Methods)].

overexpression significantly increases contact between *syd-1* mutant R7 terminals and the M6 layer (the defect is reduced by 49%; Fig. 6*A*,*B*,*D*), indicating that increased Liprin-α can partially bypass the requirement for *syd-1* during the early phase of R7 terminal development. However, Liprin-α overexpression has no effect on the later tendency of *syd-1* mutant R7s to project extensions (Fig. 6*A*,*B*,*E*); instead, the overall frequency of extensions is increased by the amount predicted given the larger proportion of terminals that contact M6 and therefore have the opportunity to extend within or beyond it. These results suggest that Syd-1 does not prevent extensions by localizing or otherwise activating Liprin-α and that therefore the early and late defects in *syd-1* mutant R7 terminal morphology are caused by different molecular mechanisms.

Previous work has shown that a second Liprin protein, Liprin-β, acts in parallel with Liprin-α in R7s (Astigarraga et al.,

2010). R7s lacking both Liprin-α and Liprin-β have a combination of the defects caused by loss of either alone: failure of their axons to contact M6 and projection of extensions beyond M6 (Astigarraga et al., 2010). The similarity of this phenotype to that caused by loss of Syd-1 suggested that, whereas Liprin-α acts downstream of Syd-1 to promote contact with M6, Liprin-β might in parallel act downstream of Syd-1 to prevent extensions. If so, we would predict that overexpressing Liprin-β in individual *syd-1*^{CD} mutant R7s would rescue the *syd-1* mutant R7 extensions. However, we found that Liprin-β overexpression had no effect on either the frequency of contact with M6 or the frequency of extensions (Fig. 6*D*,*E*), suggesting that Syd-1 does not prevent extensions by positively regulating Liprin-β.

Syd-1 acts upstream of Trio in R7s to both promote contact with M6 and prevent extensions

Trio, a GEF for Rac and Rho, is a key positive regulator of presynaptic development in fly (Ball et al., 2010). Trio overexpression rescues the R7 defects caused by loss of LAR (Maurel-Zaffran et al., 2001) and both the NMJ and R7 defects caused by loss of *Liprin-α* or *Liprin-β* (Astigarraga et al., 2010), suggesting that Trio acts downstream of these genes. We next tested whether Trio overexpression could also compensate for loss of *syd-1*. Indeed, using the *act* promoter to drive *trio* expression almost completely restores the ability of *syd-1*^{CD} mutant R7s to maintain contact with M6 (the defect is reduced by 91%; Fig. 6*C*,*D*) and significantly reduces the frequency of extensions (by 35%; Fig. 6*C*,*E*). These results suggest that *trio* acts downstream of *syd-1* during both the early and late phases of R7 terminal development and that, unlike *Liprin-α*, *trio* mediates most or possibly all of the effects of *syd-1*. If so, then loss of *trio* should resemble loss of *syd-1*. However, reducing *trio* function in R7s using RNAi was previously found only to cause extensions beyond M6 and not to disrupt the ability of R7s to contact M6 (Astigarraga et al., 2010). To remove *trio* function more completely from R7s, we created individual homozygous *trio* mutant R7s. Consistent with *trio* mediating both the early and late effects of *syd-1*, we found that *trio* mutant terminals displayed the same two morphological defects as those of *syd-1* mutant R7s: 13.9 ± 2.58% ($n = 8$ brains) of *trio*^{3} mutant R7s failed to contact the M6 layer (Fig. 7*A*), and 15.5 ± 1.94% ($n = 8$ brains) had extensions beyond M6 (Fig. 7*B*). The lower frequencies of the *trio* defects are likely caused by perdurance of wild-type Trio within *trio* mutant clones: Trio protein is expressed broadly during eye development and is required early in R neuron development for axon pathfinding (Newsome et al., 2000).

To further test whether *syd-1* and *trio* might function in the same pathway, we next tested whether *syd-1* and *trio* also have similar gain-of-function effects on R7 terminals. Overexpression of Trio has been shown previously to rescue loss of the LAR receptor phosphatase (Maurel-Zaffran et al., 2001). If *syd-1* promotes R7 terminal development by potentiating *trio* activity, then we would expect that Syd-1 overexpression should also rescue loss of *LAR*. Indeed, we found that overexpressing *syd-1* or *trio* in *LAR* mutant R7s restored contact with the M6 layer to indistinguishable degrees (the defect was reduced by 34% in both cases; Fig. 7*C*–*F*). Together, these results are consistent with a model in which the primary role of *syd-1* during both early and late phases of R7 presynaptic development is to promote *trio* activity.

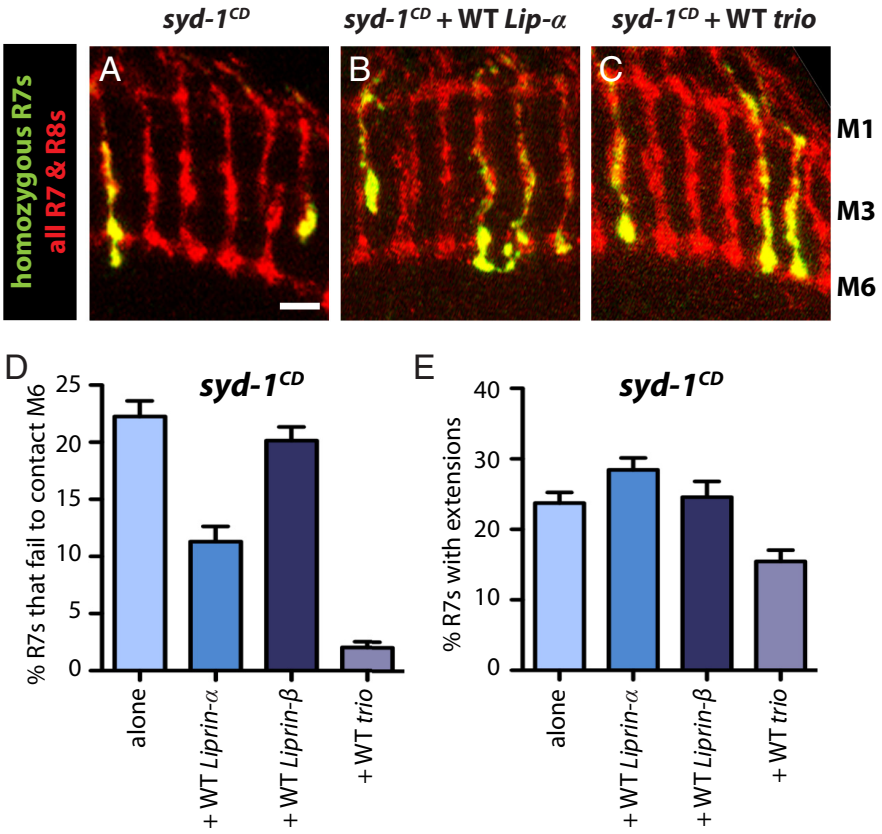

Figure 6. Overexpressing Liprin-α, Liprin-β, or Trio in *syd-1* mutant R7s rescues their defects to different degrees. ***A–C***, Medullas of adult mosaic animals in which homozygous R7s express Syt–GFP (green), and all R7 and R8 axons are labeled with mAb24B10 (red). Scale bar, 5 μm. ***A***, *syd-1*^{CD} mutant R7 axons. ***B***, Expressing *Liprin-α* in *syd-1*^{CD} mutant R7 axons partially restores their contact with M6 but does not prevent the formation of extensions. ***C***, Expressing *trio* in *syd-1*^{CD} mutant R7 axons completely restores their contact with M6 and considerably decreases the frequency of extensions. ***D***, The percentages of *syd-1*^{CD} mutant R7 axons that fail to contact M6 when overexpressing no transgene, wild-type *Liprin-α*, wild-type *Liprin-β*, or wild-type *trio*. Error bars represent SEM. This *syd-1*^{CD} mutant R7 defect (22.3 ± 1.36%; $n = 21$ brains) is partially rescued by expression of *Liprin-α* (11.3 ± 1.33%; $n = 14$ brains; $p < 0.0001$), fully rescued by expression of *trio* (2.04 ± 0.501%; $n = 15$ brains; $p < 0.0001$), and unaffected by expression of *Liprin-β* (20.1 ± 1.21%; $n = 13$ brains; $p = 0.15$). The difference between rescue by *Liprin-α* and *trio* is significant ($p < 0.0001$). ***E***, The percentages of *syd-1*^{CD} mutant R7 axons that have extensions when overexpressing no transgene, wild-type *Liprin-α*, wild-type *Liprin-β*, or wild-type *trio*. Error bars represent SEM. This *syd-1*^{CD} mutant R7 defect (23.7 ± 1.52%; $n = 21$ brains) is partially rescued by expression of *trio* (15.5 ± 1.59%; $n = 15$ brains; $p < 0.001$) but is not rescued by expression of *Liprin-α* (28.4 ± 1.70%; $n = 14$ brains; $p = 0.052$) or *Liprin-β* (24.6 ± 2.22%; $n = 13$ brains; $p = 0.38$). The difference between rescue by *Liprin-α* and *trio* is significant ($p < 0.0001$).

Discussion

Localization of SVs in R7s

GFP-fused SV proteins, such as Syt–GFP, are classic tools for studying presynaptic development but have not been used previously to analyze R7s. We found that, as expected, Syt–GFP within R7s is enriched at sites known by electron microscopy to contain active zones (Takemura et al., 2008). Loss of *LAR*, *Liprin-α*, or *syd-1* causes R7 terminals to fail to contact their normal, M6, target layer. We demonstrate here that this morphological defect correlates temporally with a failure to localize SVs to presynaptic

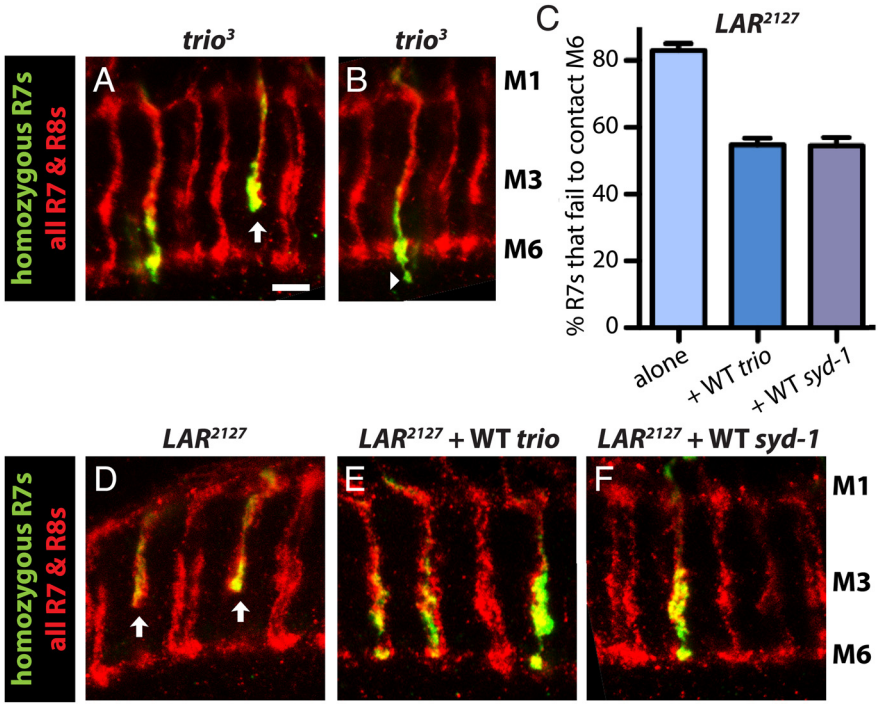

Figure 7. *trio* and *syd-1* have similar loss- and gain-of-function R7 phenotypes. ***A–F***, Medullas of adult mosaic animals in which homozygous R7s express Syt–GFP (green), and all R7 and R8 axons are labeled with mAb24B10 (red). Scale bar, 5 μm. $trio^3$ mutant R7s often fail to contact the M6 layer (***A***, arrow) and project thin extensions beyond M6 (***B***, arrowhead). $trio^1$ mutant R7s have the same two defects but at a lower frequency (data not shown). ***C***, The percentages of LAR^{2127} mutant R7 axons that fail to contact M6 when overexpressing no transgene, wild-type *trio*, or wild-type *syd-1*. Both Trio and Syd-1 significantly rescue this defect. Error bars represent SEM. The LAR^{2127} mutant R7 defect (83.0 $\pm$ 2.09%; $n = 11$ brains) is partially rescued by expression of *trio* (54.8 $\pm$ 1.99%; $n = 10$ brains; $p < 0.0001$) or *syd-1* (54.6 $\pm$ 2.37%; $n = 10$ brains; $p < 0.0001$). The difference between rescue by *syd-1* or *trio* is not significant ($p = 0.95$). ***D***, LAR^{2127} mutant R7 axons fail to contact the M6 layer (arrows). Expressing *trio* (***E***) or *syd-1* (***F***) in LAR^{2127} mutant R7 axons restores their contact with M6 to similar degrees.

sites and is therefore likely to reflect a defect in R7 presynaptic development rather than simply in target layer selection.

Liprin-α is not only a scaffold for the assembly and retention of presynaptic components, including SVs, at presynaptic sites (for review, see Stryker and Johnson, 2007) but also a positive regulator of Kinesin-3/Unc-104/Imac-dependent axon transport of those components (Shin et al., 2003; Miller et al., 2005; Wagner et al., 2009). We here show that, unlike Liprin-α, Syd-1 is not required for normal Kinesin-3/Unc-104/Imac-mediated transport. However, SVs are similarly mislocalized in *Liprin-α* and *syd-1* mutant R7 axons that contact M6. A simple interpretation is that this mislocalization reflects a requirement for *Liprin-α* and *syd-1* in retaining SVs within R7 terminals; in support of this, we found that SVs are localized normally to *syd-1* mutant R7 axon terminals at 24 h APF, before synaptogenesis. We hypothesize that the additional disruption of axon transport in *Liprin-α* mutant R7s is reflected in their greater inability to maintain contact with M6; in support of this, we found that *imac* mutant R7 axons also lose contact with M6.

Although both *Liprin-α* and *syd-1* are required for the clustering of SVs at en passant synapses in worm (Zhen and Jin, 1999; Hallam et al., 2002; Dai et al., 2006; Patel et al., 2006), *syd-1* is not required for the localization of SVs to NMJ terminals in fly (Owald et al., 2010). The molecular mechanisms underlying presynaptic development at NMJ and in R7s have been shown previously to differ in several respects (Hofmeyer and Treisman, 2009; Astigarraga et al., 2010). Our finding further highlights the importance of analyzing synapse development using multiple neuron types.

Localization of mitochondria in R7s

Although mitochondria are often enriched at synapses, it remains unclear what proportion of them might be stably associated with presynaptic sites rather than transported there in response to acute energy needs. Within at least some axons, most clusters of stationary mitochondria reside at nonsynaptic sites (Louie et al., 2008). In R7s, we found that Mito–GFP is enriched at presynaptic sites. Because arthropod photoreceptor neurons continuously release neurotransmitter in response to light (Stuart et al., 2007), this enrichment might simply be caused by continuous energy needs. However, we found that mitochondria remained enriched at R7 terminals even in the absence of light-evoked activity, indicating that either spontaneous release is sufficient for their recruitment or an activity-independent mechanism is responsible. We speculate that the permanently high energy demands at photoreceptor synapses may have selected for the activity-independent association of mitochondria with R7 synapses and that this localization requires *syd-1* and *Liprin-α*. We found that Mito–GFP is mislocalized in *imac* mutant R7s, despite previous work indicating that Kinesin-3/Unc-104/Imac is not required for transport of mitochondria (Pack-Chung et al., 2007; Barkus et al., 2008). One interpretation is that mitochondria are normally tethered at R7 presynaptic sites and that loss of *imac* indirectly causes their mislocalization by disrupting transport of the components required for tethering to occur.

Two distinct phenotypes are caused by disrupting presynaptic development in R7s

Previous work identified two different phenotypes associated with loss of the *LAR/Liprin/trio* pathway: loss of *LAR* or *Liprin-α* caused R7 axons to terminate before their M6 target layer, whereas loss of *Liprin-β* or *trio* caused R7 axons to project extensions beyond M6. One possibility is that these two defects are simply different manifestations of the same cellular defect: a decrease in the stability of the synaptic contact between R7s and their targets (Astigarraga et al., 2010). However, we have shown here that loss of a single gene, *syd-1*, causes both defects and that the defects occur at distinct developmental time points, suggesting that they occur by distinct mechanisms. In support of this, Liprin-α overexpression can rescue the early but not the late *syd-1* defect.

The earlier defect, failure to contact M6, correlates with the failure to localize SVs, suggesting, as mentioned above, that this represents a failure to assemble synapses. However, the cause of the later morphological defect and the precise nature of the extensions remain unclear. We note that the extensions often terminate in small varicosities that can contain Syt–GFP (Figs. 1*B*, 2*C*) and Mito–GFP (data not shown), indicating that they are not simply filopodia but may instead represent sites of ectopic presynaptic assembly. One possibility is that, as at NMJ (Owald et al., 2010, 2012), loss of *syd-1* causes ectopic accumulations of Liprin-α, Brp, Nrx-1, or other presynaptic proteins and that these might then promote ecto-

pic, abnormal presynaptic assembly. A second possibility is that the extensions may instead be an indirect consequence of the role of *syd-1* in postsynaptic development (Owald et al., 2010, 2012): perhaps the extensions are the response of the *syd-1* mutant R7 terminal to defects in its postsynaptic target. Loss of *Liprin-α* causes no such postsynaptic effect, providing an explanation for why *Liprin-α* mutant R7s do not form extensions. A third possibility is that R7s form distinct types of synapses at different time points. Failure to assemble one type of synapse, which R7s assemble first, causes decreased contact with M6, whereas failure to assemble a second type, which occur later, results in extensions. Consistent with this model, R7s form synapses with more than one neuron type (Gao et al., 2008; Morante and Desplan, 2008; Takemura et al., 2008).

The relationship between *syd-1* and *Liprin-α*

Loss of *syd-1* has a significantly weaker effect on fly NMJ development than does loss of *Liprin-α* (Owald et al., 2010). Likewise, here we show that the early phase of R7 terminal development, during which presynaptic components are localized, is less affected by loss of *syd-1* than by loss of *Liprin-α*. We identify a possible explanation for this difference: loss of *Liprin-α*, but not of *syd-1*, significantly decreases Kinesin-3/Unc-104/Imac-mediated axon transport, and Kinesin-3/Unc-104/Imac is required for R7s to form boutons in M6.

In both worm and fly, Syd-1 is required for the normal localization of Liprin-α and Brp/ELKS to presynaptic sites (Dai et al., 2006; Patel et al., 2006; Patel and Shen, 2009; Owald et al., 2010). In worm, loss of *syd-1* can be rescued either by overexpressing full-length wild-type Liprin-α (Dai et al., 2006; Patel et al., 2006), or by overexpressing a domain of Liprin-α that promotes oligomerization of Liprin-α proteins (Taru and Jin, 2011), or by a mutation that enhances the ability of Liprin-α to bind Brp/ELKS (Dai et al., 2006). These results suggest that the primary function of Syd-1 is to potentiate Liprin-α activities. However, we found that Liprin-α overexpression only partially rescues the early defect that *syd-1* mutant R7s have in assembling synapses. This suggests that, as in worm, Liprin-α can act partly independently of Syd-1 during presynaptic assembly but that, unlike in worm, Syd-1 also has some Liprin-α-independent function. In contrast, Liprin-α overexpression does not at all rescue the late extensions caused by loss of *syd-1*. As we speculate above, one possibility is that these extensions might be caused by mislocalized Liprin-α, Brp, or Nrx-1.

The relationship between *syd-1* and *trio*

Unlike Liprin-α, Trio overexpression fully rescues the early and partly rescues the late defect caused by loss of *syd-1*, suggesting that Syd-1 promotes R7 synaptic terminal development primarily by potentiating Trio activity. Consistent with this model, loss of *trio* phenocopies loss of *syd-1* from R7s, and overexpressing Syd-1 or Trio bypasses the need for LAR to similar degrees. At fly NMJ, Trio promotes presynaptic development by acting as a GEF for Rac1 (Ball et al., 2010). Syd-1 has a RhoGAP domain, albeit one that has not been shown to interact with GTPases (Hallam et al., 2002). Syd-1 may act distantly upstream of Trio. However, it is also possible that Syd-1 might instead regulate one or more small GTPases in parallel with Trio. GAPs and GEFs have opposite effects on GTPases, but loss of *trio* or *syd-1* causes similar defects at both NMJ and in R7s. One possibility, therefore, is that Syd-1 acts as a GAP not for Rac1 but for Rho, which often functions in opposition to Rac (Guilluy et al., 2011). Alternatively, Syd-1 might act as an atypical GAP for Rac1—perhaps lacking GAP activity but able to bind and protect Rac1–GTP from conventional GAPs—or Syd-1 might yet act as a conventional GAP for Rac1 if it is the rate of cycling between GDP- and GTP-bound states of Rac1 (rather than simply the amount of the GTPase that is in the "active," GTP-bound, state) that promotes presynaptic development.

References

Ashley JA, Katz FN (1994) Competition and position-dependent targeting in the development of the *Drosophila* R7 visual projections. Development 120:1537–1547. Medline

Astigarraga S, Hofmeyer K, Farajian R, Treisman JE (2010) Three *Drosophila* Liprins interact to control synapse formation. J Neurosci 30:15358–15368. CrossRef Medline

Ball RW, Warren-Paquin M, Tsurudome K, Liao EH, Elazzouzi F, Cavanagh C, An BS, Wang TT, White JH, Haghighi AP (2010) Retrograde BMP signaling controls synaptic growth at the NMJ by regulating Trio expression in motor neurons. Neuron 66:536–549. CrossRef Medline

Barkus RV, Klyachko O, Horiuchi D, Dickson BJ, Saxton WM (2008) Identification of an axonal Kinesin-3 motor for fast anterograde vesicle transport that facilitates retrograde transport of neuropeptides. Mol Biol Cell 19:274–283. CrossRef Medline

Berger J, Suzuki T, Senti KA, Stubbs J, Schaffner G, Dickson BJ (2001) Genetic mapping with SNP markers in *Drosophila.* Nat Genet 29:475–481. CrossRef Medline

Bloomquist BT, Shortridge RD, Schneuwly S, Perdew M, Montell C, Steller H, Rubin G, Pak WL (1988) Isolation of a putative phospholipase C gene of *Drosophila*, norpA, and its role in phototransduction. Cell 54:723–733. CrossRef Medline

Choe KM, Prakash S, Bright A, Clandinin TR (2006) Liprin-α is required for photoreceptor target selection in *Drosophila.* Proc Natl Acad Sci U S A 103:11601–11606. CrossRef Medline

Clandinin TR, Lee CH, Herman T, Lee RC, Yang AY, Ovasapyan S, Zipursky SL (2001) *Drosophila* LAR regulates R1–R6 and R7 target specificity in the visual system. Neuron 32:237–248. CrossRef Medline

Dai Y, Taru H, Deken SL, Grill B, Ackley B, Nonet ML, Jin Y (2006) SYD-2 Liprin-α organizes presynaptic active zone formation through ELKS. Nat Neurosci 9:1479–1487. CrossRef Medline

Gao S, Takemura SY, Ting CY, Huang S, Lu Z, Luan H, Rister J, Thum AS, Yang M, Hong ST, Wang JW, Odenwald WF, White BH, Meinertzhagen IA, Lee CH (2008) The neural substrate of spectral preference in *Drosophila.* Neuron 60:328–342. CrossRef Medline

Guilluy C, Garcia-Mata R, Burridge K (2011) Rho protein crosstalk: another social network? Trends Cell Biol 21:718–726. CrossRef Medline

Guo X, Macleod GT, Wellington A, Hu F, Panchumarthi S, Schoenfield M, Marin L, Charlton MP, Atwood HL, Zinsmaier KE (2005) The GTPase dMiro is required for axonal transport of mitochondria to *Drosophila* synapses. Neuron 47:379–393. CrossRef Medline

Hallam SJ, Goncharov A, McEwen J, Baran R, Jin Y (2002) SYD-1, a presynaptic protein with PDZ, C2, and RhoGAP-like domains, specifies axon identity in *C. elegans*. Nat Neurosci 5:1137–1146. CrossRef Medline

Hofmeyer K, Treisman JE (2009) The receptor protein tyrosine phosphatase LAR promotes R7 photoreceptor axon targeting by a phosphatase-independent signaling mechanism. Proc Natl Acad Sci U S A 106:19399–19404. CrossRef Medline

Hofmeyer K, Maurel-Zaffran C, Sink H, Treisman JE (2006) Liprin-α has LAR-independent functions in R7 photoreceptor axon targeting. Proc Natl Acad Sci U S A 103:11595–11600. CrossRef Medline

Kaufmann N, DeProto J, Ranjan R, Wan H, Van Vactor D (2002) *Drosophila* Liprin-α and the receptor phosphatase Dlar control synapse morphogenesis. Neuron 34:27–38. CrossRef Medline

Lee CH, Herman T, Clandinin TR, Lee R, Zipursky SL (2001) N-cadherin regulates target specificity in the *Drosophila* visual system. Neuron 30:437–450. CrossRef Medline

Lee T, Luo L (1999) Mosaic analysis with a repressible cell marker for studies of gene function in neuronal morphogenesis. Neuron 22:451–461. CrossRef Medline

Louie K, Russo GJ, Salkoff DB, Wellington A, Zinsmaier KE (2008) Effects of imaging conditions on mitochondrial transport and length in larval motor axons of *Drosophila.* Comp Biochem Physiol A Mol Integr Physiol 151:159–172. CrossRef Medline

Mahr A, Aberle H (2006) The expression pattern of the *Drosophila* vesicular glutamate transporter. Gene Expression Patterns 6:299–309. CrossRef Medline

Maurel-Zaffran C, Suzuki T, Gahmon G, Treisman JE, Dickson BJ (2001) Cell-autonomous and -nonautonomous functions of LAR in R7 photoreceptor axon targeting. Neuron 32:225–235. CrossRef Medline

McKay RR, Chen DM, Miller K, Kim S, Stark WS, Shortridge RD (1995) Phospholipase C rescues visual defect in *norpA* mutant of *Drosophila melanogaster*. J Biol Chem 270:13271–13276. CrossRef Medline

Miller AC, Seymour H, King C, Herman TG (2008) Loss of *seven-up* from *Drosophila* R1/R6 photoreceptors reveals a stochastic fate choice that is normally biased by Notch. Development 135:707–715. CrossRef Medline

Miller KE, DeProto J, Kaufmann N, Patel BN, Duckworth A, Van Vactor D (2005) Direct observation demonstrates that Liprin-α is required for trafficking of synaptic vesicles. Curr Biol 15:684–689. CrossRef Medline

Morante J, Desplan C (2008) The color-vision circuit in the medulla of *Drosophila*. Curr Biol 18:553–565. CrossRef Medline

Morey M, Yee SK, Herman T, Nern A, Blanco E, Zipursky SL (2008) Coordinate control of synaptic layer specificity and rhodopsins in photoreceptor neurons. Nature 456:795–799. CrossRef Medline

Moua P, Fullerton D, Serbus LR, Warrior R, Saxton WM (2011) Kinesin-1 tail autoregulation and microtubule-binding regions function in saltatory transport but not ooplasmic streaming. Development 138:1087–1092. CrossRef Medline

Mullins MC, Rubin GM (1991) Isolation of temperature-sensitive mutations of the tyrosine kinase receptor sevenless (*sev*) in *Drosophila* and their use in determining its time of action. Proc Natl Acad Sci U S A 88:9387–9391. CrossRef

Nern A, Nguyen LV, Herman T, Prakash S, Clandinin TR, Zipursky SL (2005) An isoform-specific allele of *Drosophila N-cadherin* disrupts a late step of R7 targeting. Proc Natl Acad Sci U S A 102:12944–12949. CrossRef Medline

Newsome TP, Schmidt S, Dietzl G, Keleman K, Asling B, Debant A, Dickson BJ (2000) Trio combines with Dock to regulate Pak activity during photoreceptor axon pathfinding in *Drosophila*. Cell 101:283–294. CrossRef Medline

Owald D, Fouquet W, Schmidt M, Wichmann C, Mertel S, Depner H, Christiansen F, Zube C, Quentin C, Korner J, Urlaub H, Mechtler K, Sigrist S (2010) A Syd-1 homologue regulates pre- and postsynaptic maturation in *Drosophila*. J Cell Biol 188:563–579. CrossRef

Owald D, Khorramshahi O, Gupta VK, Banovic D, Depner H, Fouquet W, Wichmann C, Mertel S, Eimer S, Reynolds E, Holt M, Aberle H, Sigrist SJ (2012) Cooperation of Syd-1 with Neurexin synchronizes pre- with postsynaptic assembly. Nat Neurosci 15:1219–1226. CrossRef Medline

Pack-Chung E, Kurshan PT, Dickman DK, Schwarz TL (2007) A *Drosophila* Kinesin required for synaptic bouton formation and synaptic vesicle transport. Nat Neurosci 10:980–989. CrossRef Medline

Parks AL, Cook KR, Belvin M, Dompe NA, Fawcett R, Huppert K, Tan LR, Winter CG, Bogart KP, Deal JE, Deal-Herr ME, Grant D, Marcinko M, Miyazaki WY, Robertson S, Shaw KJ, Tabios M, Vysotskaia V, Zhao L, Andrade RS, et al. (2004) Systematic generation of high-resolution deletion coverage of the *Drosophila melanogaster* genome. Nat Genet 36:288–292. CrossRef Medline

Patel MR, Shen K (2009) RSY-1 is a local inhibitor of presynaptic assembly in *C. elegans*. Science 323:1500–1503. CrossRef Medline

Patel MR, Lehrman EK, Poon VY, Crump JG, Zhen M, Bargmann CI, Shen K (2006) Hierarchical assembly of presynaptic components in defined *C. elegans* synapses. Nat Neurosci 9:1488–1498. CrossRef Medline

Pearn MT, Randall LL, Shortridge RD, Burg MG, Pak WL (1996) Molecular, biochemical, and electrophysiological characterization of *Drosophila norpA* mutants. J Biol Chem 271:4937–4945. CrossRef Medline

Rao S, Lang C, Levitan ES, Deitcher DL (2001) Visualization of neuropeptide expression, transport, and exocytosis in *Drosophila melanogaster*. J Neurobiol 49:159–172. CrossRef Medline

Riesgo-Escovar J, Raha D, Carlson JR (1995) Requirement for a phospholipase C in odor response: Overlap between olfaction and vision in *Drosophila*. Proc Natl Acad Sci U S A 92:2864–2868. CrossRef Medline

Schindelin J, Arganda-Carreras I, Frise E, Kaynig V, Longair M, Pietzsch T, Preibisch S, Rueden C, Saalfeld S, Schmid B, Tinevez JY, White DJ, Hartenstein V, Eliceiri K, Tomancak P, Cardona A (2012) Fiji: an open-source platform for biological-image analysis. Nat Methods 9:676–682. CrossRef Medline

Sellers VM, Wang KF, Johnson MK, Dailey HA (1998) Evidence that the fourth ligand to the [2Fe-2S] cluster in animal ferrochelatase is a cysteine. Characterization of the enzyme from *Drosophila melanogaster*. J Biol Chem 273:22311–22316. CrossRef Medline

Shin H, Wyszynski M, Huh KH, Valtschanoff JG, Lee JR, Ko J, Streuli M, Weinberg RJ, Sheng M, Kim E (2003) Association of the Kinesin motor KIF1A with the multimodular protein Liprin-α. J Biol Chem 278:11393–11401. CrossRef Medline

Stowers RS, Schwarz TL (1999) A genetic method for generating *Drosophila* eyes composed exclusively of mitotic clones of a single genotype. Genetics 152:1631–1639. Medline

Stryker E, Johnson KG (2007) LAR, liprin α and the regulation of active zone morphogenesis. J Cell Sci 120:3723–3728. CrossRef Medline

Stuart AE, Borycz J, Meinertzhagen IA (2007) The dynamics of signaling at the histaminergic photoreceptor synapse of arthropods. Prog Neurobiol 82:202–227. CrossRef Medline

Takemura SY, Lu Z, Meinertzhagen IA (2008) Synaptic circuits of the *Drosophila* optic lobe: the input terminals to the medulla. J Comp Neurol 509:493–513. CrossRef Medline

Taru H, Jin Y (2011) The Liprin homology domain is essential for the homomeric interaction of SYD-2/Liprin-α protein in presynaptic assembly. J Neurosci 31:16261–16268. CrossRef Medline

Ting CY, Yonekura S, Chung P, Hsu SN, Robertson HM, Chiba A, Lee CH (2005) *Drosophila* N-cadherin functions in the first stage of the two-stage layer-selection process of R7 photoreceptor afferents. Development 132:953–963. CrossRef Medline

Ting CY, Herman T, Yonekura S, Gao S, Wang J, Serpe M, O'Connor MB, Zipursky SL, Lee CH (2007) Tiling of R7 axons in the *Drosophila* visual system is mediated both by transduction of an Activin signal to the nucleus and by mutual repulsion. Neuron 56:793–806. CrossRef Medline

Wagner OI, Esposito A, Köhler B, Chen CW, Shen CP, Wu GH, Butkevich E, Mandalapu S, Wenzel D, Wouters FS, Klopfenstein DR (2009) Synaptic scaffolding protein SYD-2 clusters and activates kinesin-3 UNC-104 in *C. elegans*. Proc Natl Acad Sci U S A 106:19605–19610. CrossRef Medline

Wernet MF, Mazzoni EO, Celik A, Duncan DM, Duncan I, Desplan C (2006) Stochastic Spineless expression creates the retinal mosaic for colour vision. Nature 440:174–180. CrossRef Medline

Yeh E, Gustafson K, Boulianne GL (1995) Green fluorescent protein as a vital marker and reporter of gene expression in *Drosophila*. Proc Natl Acad Sci U S A 92:7036–7040. CrossRef Medline

Zhang YQ, Rodesch CK, Broadie K (2002) Living synaptic vesicle marker: synaptotagmin-GFP. Genesis 34:142–145. CrossRef Medline

Zhen M, Jin Y (1999) The liprin protein SYD-2 regulates the differentiation of presynaptic termini in *C. elegans*. Nature 401:371–375. CrossRef Medline